NASA Contractor Report 174836

Viscoplastic Constitutive Relationships with Dependence on Thermomechanical History

D.N. Robinson and P.A. Bartolotta

The University of Akron
Akron, Ohio

March 1985

Prepared for

NATIONAL AERONAUTICS AND SPACE ADMINISTRATION
Lewis Research Center
Under Contract NAG 3-379

INTRODUCTION

Essentially all of the important structural problems related to the design of high-temperature energy system components, e.g., aircraft and rocket engine components, and nuclear reactor system components, are non-isothermal. Inelasticity does not occur in these components as a result of mechanical loading alone but is induced mainly through thermal transient cycles and thermal gradients. Nevertheless, the constitutive equations and damage models used in structural analysis and design are almost always based completely on experimental data collected under isothermal conditions. Isothermal tests are commonly conducted over the temperature range of interest; material "constants" are determined at each test temperature and then "fit" as functions of temperature across the temperature range to furnish a "nonisothermal" representation. This approach fails to reflect the strong thermomechanical path dependence observed in, for example, the cyclic hardening behavior of some alloys of interest - particularly in the presence of metallurgical changes (refs. 1 - 4).

Not only are constitutive relationships used in large scale structural analysis often based solely on isothermal data but, further, they often represent only saturated cyclic behavior. As many common alloys continue to cyclically harden over several hundred or even several thousand cycles (ref. 1-4), and, as many large scale inelastic analyses are carried out only over a few cycles (largely for economic reasons), it is essential to characterize cyclic hardening over a wide range of cycling - not just for saturated conditions.

VISCOPLASTIC CONSTITUTIVE RELATIONSHIPS WITH DEPENDENCE ON THERMOMECHANICAL HISTORY‡

D. N. Robinson*
P. A. Bartolotta**

ABSTRACT

Experimental evidence of thermomechanical history dependence in the cyclic hardening behavior of some common high-temperature structural alloys is presented with special attention paid to the contribution of dynamic metallurgical changes. A discussion is given concerning the inadequacy of formulating "nonisothermal" constitutive equations solely on the basis of isothermal testing.

A representation of thermoviscoplasticity is proposed that qualitatively accounts for the observed hereditary behavior. This is achieved by formulating the scalar evolutionary equation in an established viscoplastic theory to reflect thermomechanical path dependence. Although the necessary nonisothermal tests for further quantifying the thermoviscoplastic model have been identified, such data are not yet available.

To assess the importance of accounting for thermomechanical history dependence in practical structural analyses, two qualitative models are specified; the first is formulated as if based entirely on isothermal information, as is most often done; the second is made to reflect thermomechanical path dependence using the proposed thermoviscoplastic representation. Comparisons of predictions of the two models are made and a discussion is given of the impact the calculated differences in deformation behavior may have on subsequent lifetime predictions.

‡ This research was sponsored by NASA/Lewis Research Center, Cleveland, Ohio under Grant NAG-3-379.

* Professor, Department of Civil Engineering, University of Akron, Akron, Ohio.

** Graduate Student, Department of Civil Engineering, and NASA/University of Akron Fellow, University of Akron, Akron, Ohio.

In this paper, we address thermomechanical path dependence in cyclic hardening with special emphasis on that induced through metallurgical changes e.g., through dynamic strain aging. Definitive phenomenological evidence of thermomechanical history dependence is cited and a heuristic discussion is given of its microscopic origin in solid solution hardening alloys. Related thermomechanical hereditary behavior is found in two-phase superalloys (ref. 5) arising from precipitation of the γ' phase.

A mathematical representation of thermoviscoplasticity is proposed that qualitatively accounts for the observed hereditary behavior. This is accomplished by appropriately formulating the evolutionary equation for the scalar state variable in a viscoplastic model developed principally by Robinson (refs. 6,7) to reflect thermomechanical path dependence. Although candidate nonisothermal tests providing the necessary information to further quantify the thermoviscoplastic model have been identified, they will not be conducted until the presently expanding Structures Division Laboratory at NASA/Lewis Research Center becomes operative.

To assess the importance of accounting for thermomechanical history in practical applications, two (qualitative) models are specified; one is taken as if based entirely on isothermal information as is traditionally done, and the second is taken to reflect thermomechanical path dependence using the representation proposed in the present work. Applications of each model are made to homogeneously stressed elements under some prescribed thermomechanical histories and the results are compared.

THERMOMECHANICAL HISTORY DEPENDENCE AND METALLURGICAL CHANGE

It is well known that cyclic hardening of some structural alloys within their temperature range of interest is influenced by the phenomenon of dynamic strain aging (ref 8). Strain aging occurs in solid solutions

where solute atoms are particularly free to diffuse through the parent lattice. It is energetically preferable for these solute atoms to occupy sites in the neighborhood of mobile dislocations where their presence immobilizes the dislocations or at least makes their movement difficult, thus causing strengthening.

Isothermal cycling at temperatures where such metallurgical changes occur might therefore be expected to show abnormal hardening, i.e., higher hardening rates and greater saturation strengths than at temperatures both lower and higher. Evidence of strain aging in type 304 stainless steel is indicated in figure 1 (solid curves). There, the hardening rate and "saturation" strength are seen to be greatest at the intermediate temperature 593C (1100F). Figure 2 shows the same behavior in the nickel-based alloy Hastelloy X (solid curves) at the specified strain range and rate and in the temperature range 427-649C (800-1200F). In this case the hardening rate and strength are greatest for the highest temperature 649C (1200F). For temperatures greater than 649C (not shown) both the hardening rate and saturation strength decrease markedly. Similar behavior is observed in type 316 stainless steel in figure 3. Further evidence of dynamic strain aging is reported in ref. 1-4.

The observed hardening peak in these examples is interpreted as a manifestation of dynamic strain aging. At lower temperatures the mobility of solute atoms is far less and strain aging does not occur; at higher temperatures normal recovery processes, e.g., climb of edge dislocations, take over.

In the aging process described dislocations can break away from their "Cottrell solute atmospheres" becoming mobile again. Although temporarily freed, dislocations can again be immobilized as solute atoms gradually

diffuse back to them. As the thermally activated process of diffusion is involved and solute atoms are migrating to dislocations which themselves are moving under the applied stress, it is not surprising that the ensuing inelastic deformation (cyclic hardening in particular) has a complex dependence on thermomechanical history.

Phenomenological evidence of thermomechanical path dependence under cyclic conditions is seen in the results of the simple stepwise nonisothermal tests reported in figure 1 and 2 (dotted curves). In these tests cycling is initiated at one temperature, after which the temperature is changed and cycling resumed.

Figure 1 shows the result of a nonisothermal test on type 304 stainless steel in which cycling is initiated at 427C (800F) for about fifty cycles; the temperature is then changed to 593C (1100F) and cycling continued (dotted curve). Note that the material softens with the temperature increase, contrary to the implication of the isothermal hardening data. Hardening continues to 1000 cycles, however the stress amplitude remains measurably less than that indicated by the 593C isothermal curve.

Figure 2 includes the results of four stepwise nonisothermal tests on Hastelloy X (dotted curves). Test path oabc represents the response to cycling at 649C (1200F) to 800 cycles and then at 427C (800F) to 2000 cycles. Test odef represents cycling at 649C (1200F) to 1600 cycles followed by cycling at 427C (800F) to 2000 cycles. Path oghj shows cycling to 1600 cycles at 427C (800F) where the temperature is brought to 649C (1200F) and cycling continued. Finally, the two step test okmnps is reported. Here, cycling starts at 427C (800F) to 800 cycles, is changed to 649C (1200F) through 1200 cycles and then back to 427C (800F) to 2000 cycles. Note that the points f, c, s and 4 in figure 2 all represent the cyclic strength

(stress range) at 427C (800F) and 2000 cycles, the distinction being that each is reached over a different thermomechanical path. The range of "saturation" strengths at 427C (800F) is close to 200 MPa. Similarly, points 1 and j in figure 2 correspond to 649C (1200F) strengths at 2000 cycles following different thermomechanical histories.

The features of these test results that reflect thermomechanical history dependence are:

1) The change in strength (stress range) with temperature at a fixed number of cycles is always negative, i.e., an increase in temperature always results in a decrease in strength and vice versa - contrary to the implications of the isothermal data;
2) The strength, in particular the "saturation" strength, depends on the temperature-strain history. The data suggest that the material retains a full memory of the thermomechanical path to cyclic saturation. Evidently, the information contained in the isothermal data is not sufficient to predict the hardening behavior under nonisothermal conditions.

REPRESENTATION OF THERMOVISCOPLASTIC CYCLIC HARDENING

It is assumed in the following that the gradual hardening (or softening) that accumulates over several cycles under cyclic stressing occurs isotropically and therefore can be described in terms of a single scalar state variable. That is not to say that kinematic (induced anisotropic) effects are not strongly present during cycling as the internal dislocation structure alters with immobilization and remobilization of dislocations under repeated stress reversals. Kinematic features are modeled through a tensorial state variable commonly identified as the internal or back stress.

The flow law in the viscoplastic theory of refs. 6 and 7 is written (see Appendix):

$$2\mu\dot{\varepsilon}_{ij} = f(F)\,\frac{\sum_{ij}}{\sqrt{J_2}} \tag{1}$$

in which $\dot{\varepsilon}_{ij}$ denotes the components of inelastic strain-rate, μ is a material parameter, f and F are material functions and J_2 is the second principal invariant of the effective stress

$$\sum_{ij} = s_{ij} - a_{ij} \tag{2}$$

as defined in the Appendix.

For an initially isotropic material, the stress dependence enters through

$$F = \frac{J_2}{k^2} - 1 \tag{3}$$

F plays the role of a Bingham-Prager yield function in which k denotes the Bingham threshold shear stress below which the inelastic strain rate vanishes. In this state variable description k is a scalar state variable accounting for isotropic hardening effects and α_{ij} are the components of a tensorial state variable (internal stress) accounting for kinematic effects.

As the experimental work cited here is uniaxial we write equation (3) in uniaxial terms using

$$J_2 = \frac{(\sigma-\alpha)^2}{3} \tag{4}$$

thus

$$F = \frac{(\sigma-\alpha)^2}{K} - 1 \tag{5}$$

where $K=3k^2$. σ and α denote the uniaxial components of the applied and internal (back) stress. Our concern in this study reduces to the specification of an appropriate form of evolutionary law for K in equation (5) that reflects the thermomechanically hereditary behavior observed in figs. 1-3 and cited in refs. 1-4.

In the subsequent development we take isotropic hardening, through K, to depend on inelastic work

$$W = \int s_{ij} d\varepsilon_{ij}, \tag{6}$$

however, the formulation is not innately limited to dependence on W and could, if appropriate, be taken to depend on some other scalar measure of mechanical deformation, say,

$$P = \int \sqrt{d\varepsilon_{ij} d\varepsilon_{ij}} \tag{7}$$

the accumulated plastic strain.

It is supposed that a typical material of concern cyclically hardens under some fixed strain range and strain rate as shown schematically in fig. 4. This is qualitatively in keeping with the actual material response observed in figs. 1-3 and with the physical arguments made in the previous section. Fig. 4a can be interpreted as a plot of $\Delta\sigma$ vs N (stress range vs number of cycles) or K vs W for isothermal cycling (solid curves) at the three temperatures $T_1<T_2<T_3$. Fig. 4b which is a plot of $\Delta\sigma$ or K vs temperature T shows the commonly observed "strain-aging peak".

Classically, K has been taken as an explicit function of W and T, (e.g., ref. 9). This implies the existence of a unique surface K(W,T) as in fig. 4c that can be determined fully on the basis of isothermal hardening curves. This is equivalent to adopting the evolutionary equation for K as

$$dK = \frac{\partial K}{\partial W} dW + \frac{\partial K}{\partial T} dT \tag{8}$$

which is a perfect differential and integrable independently of the thermomechanical path W(T) as illustrated in fig. 4c. A candidate representation of the isothermal curves of figs. 4a and 4b and the surface K(W,T) in fig. 4c is:

$$K(W,T) = K_s(T) + [K_i(T) - K_s(T)]e^{-W/W_o(T)} \tag{9}$$

The functions $K(0,T)=K_i(T)$ and $K(\infty,T)=K_s(T)$ are as illustrated in fig. 4b. The function $W_o(T)$ determines the temperature dependent cyclic hardening rate.

The classical representation described above clearly does not reflect the thermomechanical path dependence apparent in the test data of figs. 1-3 or in the schematically represented nonisothermal responses of fig. 4a (dotted curves). In particular, the saturated strength in the classical description depends only on the current temperature, i.e., $K_{s(T)}$, and is

thus independent of the thermomechanical path leading to saturation. Actual data shows that the saturation strength does significantly depend on thermal-strain history. Furthermore, the classical description permits an increase in strength with an increase in temperature in the neighborhood of the "strain-aging peak" (fig. 4b). Nonisothermal data shows that an increase in temperature is always accompanied by a decrease in strength, i.e., a decrease in K.

A form of evolutionary equation for K in equation (5) that does allow for thermomechanical history dependence of the cyclic hardening response is the following:

$$dK = \Gamma(W,T)dW + \theta(W,T)dT \tag{10}$$

Equation (10) represents a kinetic growth law for K which is not a perfect differential and is integrable only when the thermomechanical path W(T) is known*. The functions $\Gamma(W,T)$ and $\theta(W,T)$ are independent and not related as $\partial K/\partial W$ and $\partial K/\partial T$ are in equation (8). The function $\Gamma(W,T)$ can be determined on the basis of isothermal testing whereas $\theta(W,T)$ cannot. A complete description of the nonisothermal hardening behavior in terms of equation (10) necessarily involves nonisothermal testing.

Candidate nonisothermal tests providing definitive information about the function $\theta(W,T)$ have been identified and are included in the test plan for the currently expanding Structures Division Laboratory at NASA Lewis Research Center. For present purposes the results of related tests, identified earlier (refs. 1,2) by D. N. Robinson and conducted by R. W. Swindeman at Oak Ridge National Laboratory on types 304 and 316 stainless steel, have been us

---

* It may be appropriate under some circumstances to account for thermal recovery effects in the evolutionary law for K. As the emphasis here is on thermomechanical history effects, particularly in accompaniment of metallurgical changes that occur at intermediate temperatures, we ignore thermal recovery in K.

in suggesting an appropriate qualitative form of $\theta(W,T)$, and similarly of $\Gamma(W,T)$. On that basis we propose the following functional forms of Γ and θ in the evolutionary equation (10):

$$\Gamma(W,T) = \left(\frac{K_s(T) - K_i(T)}{W_o(T)} \right) e^{-W/W_o(T)} \tag{11}$$

$$\theta(W,T) = - \frac{Q(W)}{T^2} e^{-Q(W)(1/T_o - 1/T)} \tag{12}$$

where W is the inelastic work as defined in equation (6) and T is the absolute temperature.

Note that Γ is identical to $\partial K/\partial W$ in equation (8) with K taken as in equation (9). Thus the functions K_i, K_s and W_o play the same roles as described earlier in the classical representation. However, the Arrhenius form adopted for θ is not equal to $\partial K/\partial T$ in equation (8). The "activation energy" Q is, as yet, an unspecified function of W and T_o is a reference temperature.

For isothermal cycling at a fixed temperature T, we have $dT = 0$ and equation (10) integrates to equation (9). Thus, the classical representation where K in equation (5) is taken as an explicit function of W and T, (i.e., equation (9)), and the present formulation based on the evolutionary law expressed in equations (10) - (12) give identical results under isothermal conditions.

With temperature changes in the absence of mechanical deformation, i.e., with $dW = 0$, equation (10) gives

$$\frac{dK}{dT} = \theta(W,T) = - \frac{Q(W)}{T^2} e^{-Q(W)(1/T_o - 1/T)} \tag{13}$$

which, for $Q(W)>0$, ensures that

$$\frac{dK}{dT} < 0 \tag{14}$$

for all W and T - in keeping with the experimental observations cited above and contrary to the predictions based on the classical formulation.

A finite temperature change from the reference temperature T_0 to T in the undeformed (W=0) state causes a change in $K(=K_i)$ found by integrating equation (13)

$$\int_{K_0}^{K_i(T)} dK = \int_{T_0}^{T} -\frac{Q_0}{T^2} e^{-Q_0(1/T_0 - 1/T)} \, dT \qquad (15)$$

in which $K_0 = K_i(T_0)$ and $Q_0 = Q(0)$. Equation (15) integrates to

$$K_i(T) = K_0 - (1 - e^{-Q_0(1/T_0 - 1/T)}) \qquad (16)$$

The Arrhenius temperature dependence for K_i (initial strength) is substantiated in biaxial (tension-torsion) experiments conducted on type 316 stainless steel (ref. 10).

A critical feature of the evolutionary law expressed in equations (10)-(12) is that it permits the cyclic hardening, in particular the saturated strength, to be dependent on thermomechanical history. This feature will be explored in more detail in the following sections.

SPECIFICATION OF TWO CYCLIC HARDENING MODELS FOR COMPARISON

In this section we formulate two models for qualitatively describing the cyclic hardening behavior discussed above. Each is based on the viscoplastic constitutive equations outlined in the Appendix. The first, Model A, adopts

the "classical" representation of cyclic hardening identified in the preceding section and is treated as if based entirely on isothermal testing. The second model, Model B, is based on the thermoviscoplastic representation outlined in the last section and is taken as being based on nonisothermal experimentation. Although, as indicated earlier, definitive nonisthermal data are not presently available, some qualitative guidance has been provided in formulating Model B from preliminary tests conducted at Oak Ridge National Laboratory.

Predictions will be made using each model and compared in an effort to assess the importance of accounting for thermomechanical path dependence in practical applications.

The details of the formulation of each of the models will now be given.

1. Model A

Constitutive model A assumes that the state variable K in equation (5) is an explicit function of W and T, namely, that given by equation (9).

The function $K_i(T)$ in equation (9) is taken as specified in equation (16) with

$$K_0 = 2$$

$$Q_0 = 4000 \qquad (17)$$

and $$T_0 = 800 \text{ K}$$

The functions $K_S(T)$ and $W_0(T)$ are, respectively

$$K_S(T) = A + B(T-T_p) + C(T - T_p)^2 \qquad (18)$$

with $A = 16$

$B = -0.04$ (19)

$C = -0.001$

and $W_o(T) = \overline{A} + \overline{B}(T-T_p)^2$ (20)

with $\overline{A} = 0.5$

$\overline{B} = 5x10^{-5}$ (21)

In each case $T_p = 700$ K .

Isothermal curves K vs W for model A based on equation (9) and equations (17) -(21) are shown in fig. 5a (solid curves). These represent hardening at 600K, 700K and 800K. Fig. 5b shows the curves $K(0,T) = K_i(T)$ and $K(\infty,T) = K_s(T)$. The curves in figs. 5a and 5b agree with the schematic representation in figs. 4a and 4b, including the appearance of the "strain aging peak". Note that the surface K(W,T) defined by the solid curves in figs. 5a and 5b is unique in the case of Model A, and K remains on this surface for all thermomechanical paths as schematically illustrated in fig. 4c. Thus, Model A does not reflect thermomechanical path dependence.

2. Model B

Model B incorporates the kinetic growth law given in equations (10) - (12). The functions $K_i(T)$, $K_s(T)$ and $W_o(T)$ in $r(W,T)$[equation (11)] are taken identical to those defined for model A. Although a exact form of the "activation energy" Q(W) in equation (12) is not presently known, data in ref.(1,2) on type 304 stainless steel suggest it may not be a strong function of W. With that as a guide we choose Q to be a constant until appropriate test data become available, i.e. we take $Q(W) = Q(0) = Q_o$. The value of Q_o has previously been specified in equation (17).

The isothermal K vs W curves for model B are, of course, identical to those for model A and likewise appear as the solid curves in figs. 5a and 5b. Now, however, thermomechanical paths other than isothermal ones do not necessarily remain on the surface defined by the isothermal data. This is illustrated by the calculated curves (dotted lines) in fig. 5a depicting nonisothermal cycling based on Model B. These are in qualitative agreement with the experimental responses observed in figs. 1 and 2.

The calculations made using either model A or B require coupling with a representation of linear thermoelasticity. As all calculations are uniaxial and assume initial isotropy, it suffices to specify only the Young's modulus E and the linear coefficient of expansion α_t. Thus:

$$E(T) = 4x10^4 - 21.6\ T \tag{22}$$

$$\alpha_t = 14 \times 10^{-6} \tag{23}$$

giving E in ksi and α_t in K^{-1}. Here only E is taken to depend on temperature.

The two models formulated above, each based on the viscoplastic model stated in the Appendix, are valid within the following range of absolute temperature.

$$600K < T < 800K.$$

This completes the specification of the two models A and B.

PREDICTIONS BASED ON MODELS A AND B

We first consider predictions of uniaxial isothermal cycling over a fixed strain range and strain rate. Figures 6,7, and 8 show predicted isothermal stress-strain loops for cycling over a strain

range of $\Delta e = \pm 0.25\%$ and a strain rate of $\dot{e} = 0.4$ %/m at the temperatures 600K, 700K and 800K respectively. The hardening rate and saturation strength are evidently greatest for the intermediate temperature 700K, as is typical of solid solution alloys that exhibit strain aging. The predicted isothermal hysteresis loops are identical for models A and B. A plot of stress amplitude $\Delta\sigma$ versus the number of stress reversals 2N corresponding to the isothermal hysteresis loops of figs. 6 - 8 is shown in figure 9 (solid curves).

For thermomechanical paths other than isothermal ones, models A and B show qualitatively different behavior. For example, consider cycling at 600K over the path O_1a in figure 9. At point a we suppose the temperature to be changed to 700K and cycling continued. The predicted response according to model A is an increase in $\Delta\sigma$ to the point c at the next reversal and then to saturation at S_2 under continued cycling. The stress amplitude S_2 is precisely that at which saturation occurs for isothermal cycling at 700K. The prediction of model B, on the other hand, follows the path abS_4. This shows a decrease in strength to b with the temperature increase, qualitatively in keeping with experimental observations, and saturation at S_4, considerably different than S_2; this too, is in accordance with experiments. Other predicted paths based on model B are O_2deS_5 and O_3ghS_6. The former corresponds to cycling first at 700K (O_2d) then changing to 600K (eS_5). The latte involves cycling at 800K(O_3g) followed by cycling at 700K (hS_6) with saturation occuring at S_6. Note that saturation at the temperature 700K occurs in these predictions based on model B at S_2, S_4 or S_6 depending upon the thermo mechanical path.

We next consider thermomechanical cycling as illustrated in figure 10. Here, a uniaxial specimen is supposed to be initially at 600K in its virgin (zero stress-zero strain) state. The total strain is held zero while

the temperature is cycled between 600K and 800K. Predictions of stress versus mechanical strain corresponding to a temperature ramp rate of 5K/sec are shown in figures 11, 12 and 13. Figure 11 shows the response based on model A; figure 12 shows that predicted from model B. Figure 13 is based on model A using only saturated isothermal data, i.e., taking $K = K_S(T)$ in Eq.(5), as is commonly done in practice.

The limit cycles in figs. 11(or 13) and 12 are measurably different. The shape in figure 12 calculated using model B appears far more representative of the results of generic experiments of this type (ref. 2). The difference in subsequent life predictions based on the two stable loops is speculative at present. Based on intuition developed for isothermal cycling one might expect the two lifetime predictions to be not too different since the inelastic strain range (width of the loops) and the stress values at the extremities of the loops are not drastically different. Nevertheless, the deformation prediction based on isothermal information alone (model A) does tend to indicate a narrower loop and thus might be expected to give the longer estimate of lifetime. Of course, such calculations depend strongly on the particular lifetime model being employed.

Figures 14, 15 and 16 represent the same test as in the previous three figures except with the temperature ramp rate increased by an order of magnitude to 50K/sec. This calculation is made mainly to demonstrate the rate dependency of the viscoplastic constitutive model and the influence this has on thermomechanical response. Comparing the limit cycles in figure 14 or 16 (model A) and figure 15 (model B) we see that their differences tend to be further exaggerated at the higher strain rate. Here, model A appears even more likely to give the less conservative estimate of lifetime.

The results of a final calculation are shown in figure 17. We again consider the problem illustrated in figure 10 but with the maximum temperature taken as 700K instead of 800K. The temperature rate is 5K/sec. In figure 17 we compare the stable hysteresis loops based on model A, in which just saturated isothermal information is considered, and model B. The responses are now vastly different. Model A predicts shakedown (elastic cycling) about a sizable compressive mean stress. Model B does not show shakedown; its stable loop has finite width. Furthermore, the model B prediction indicates a far more damaging tensile mean stress. Here again, the trend is for the model based only on isothermal information (model A) to give the least nonconservative lifetime prediction.

SUMMARY AND CONCLUSIONS

Experimental evidence of thermomechanical history dependence in the cyclic hardening behavior of some structural alloys of interest is cited with particular emphasis on the contribution of dynamic metallurgical changes. On this basis a discussion is given of the inadequacy of formulating "nonisothermal" constitutive relationships solely on the basis of isothermal test data, as is often done in practice.

A representation of thermoviscoplasticity is proposed that qualitatively accounts for the observed hereditary cyclic hardening behavior. This is accomplished by appropriately reformulating the evolutionary equation for the scalar state variable in an established viscoplastic theory to reflect thermomechanical path dependence. Although the necessary nonisothermal tests for further quantifying the thermoviscoplatic model have been tentatively identified, such data are not yet available.

To assess the importance of accounting for thermomechanical history dependence in practical structural analyses, two qualitative models are specified; the first is formulated as if based entirely on isothermal information, as is commonly the case; the second is made to reflect thermomechanical path dependence using the thermoviscoplastic representation proposed here. Comparisons of predictions of the two models are made and a speculative discussion is given of the impact the calculated differences in deformation behavior may have on subsequent lifetime predictions.

Conclusions drawn from the present study are as follows:

- Cyclic hardening occurs over a few thousand cycles in the alloys addressed here and for the strain ranges and rates considered. At lesser strain ranges hardening may continue over several thousand cycles. Therefore, a meaningful representation of cyclic deformation behavior should not be based solely on cyclically saturated strength, as is commonly the case.
- The information contained in isothermal cyclic hardening data is not sufficient to predict hardening behavior under general thermomechanical conditions.
- For the common alloys considered here, it appears that the saturation strength under cyclic conditions depends on the thermomechanical history to saturation, particularly in presence of metallurgical changes.
- The thermoviscoplastic representation presented here qualitatively accounts for the thermomechanical path dependence observed in the simple nonisothermal tests cited.

- Comparison of predicted results of the two qualitative models indicated above under some simple thermomechanical loadings suggest that subsequent lifetime predictions may tend to be "nonconservative" when based on "nonisothermal" models formulated solely from isothermal data.

REFERENCES

1. Robinson, D.N. and Swindeman, R.W., "Additions and Modifications to Constitutive Equations in NE Standard F9-5T," High-Temperature Structural Design Program Prog. Rep., ORNL-5794, June 1981.

2. Robinson, D.N. and Swindeman, R.W., "Modifications to Constitutive Equations in NE Standard F9-5T," High-Temperature Structural Design Program Prog. Rep., ORNL-5863, Dec. 1981.

3. Robinson, D.N., "Thermomechanical Deformation in the Presence of Metallurgical Changes," Proc. Second Symposium on Nonlinear Constitutive Relations for High Temperature Applications, NASA Lewis Research Center Cleveland, Ohio, NASA Conf. Pub. 2271, June 1984.

4. Robinson, D.N., and Ellis, J.R., "High-Temperature Constitutive Modeling," Proc. Conf. on Turbine Engine Hot Section Technology, NASA Lewis Research Center, Cleveland, Ohio, NASA Conf. Pub. 2339, Oct. 1984.

5. Cailletaud, G. and Chaboche, J.-L., "Macroscopic Description of the Microstructural Changes Induced by Varying Temperature: Example of IN 100 Cyclic Behavior," ICM, 3, Vol. 2, 1979.

6. Robinson, D.N., "A Unified Creep-Plasticity Model for Structural Metals at High Temperature," ORNL/TM 5969, November 1978.

7. Robinson, D.N. and Swindeman, R.W., "Unified Creep-Plasticity Constitutive Equations for Structural Alloys at Elevated Temperature," ORNL/TM 8444, October 1982.

8. Baird, J.D., "Dynamic Strain Aging," The Inhomogeneity of Plastic Deformation, ASM, Metals Park, Ohio, 1973.

9. "Guidelines and Procedures for Design of Nuclear System Components at Elevated Temperature", NE (RDT) Standard F9-5T, U.S. Energy Research and Development Administration, September 1974.

10. Reid, S.R. and Ellis, J.R., "Multiaxial Exploratory Testing," High-Temperature Structural Design Program Prog. Rep., ORNL/5737, Dec. 1980.

APPENDIX

Here we state the viscoplastic constitutive equations of ref. 6 and 7 in nonisothermal and multiaxial form. As written, the equations are valid for "small" deformations and initially isotropic materials.

$$2\mu\dot{\varepsilon}_{ij} = \begin{cases} \dfrac{F^n \Sigma_{ij}}{\sqrt{J_2}} & ; \quad F > 0 \text{ and } S_{ij}\Sigma_{ij} > 0 \\ 0 & ; \quad F \leq 0 \quad \text{or} \\ & \quad F > 0 \text{ and } S_{ij}\Sigma_{ij} \leq 0 \end{cases} \tag{1A}$$

$$\dot{a}_{ij} = \begin{cases} \dfrac{H}{G^\beta}\dot{\varepsilon}_{ij} - RG^{m-\beta}\dfrac{a_{ij}}{\sqrt{I_2}} & ; \quad G > G_o \text{ and } S_{ij}a_{ij} > 0 \\ \dfrac{H}{G_o^\beta}\dot{\varepsilon}_{ij} - RG_o^{m-\beta}\dfrac{a_{ij}}{\sqrt{I_2}} & ; \quad G \leq G_o \text{ or } S_{ij}a_{ij} \leq 0 \end{cases} \tag{2A}$$

in which,

$$\Sigma_{ij} = S_{ij} - a_{ij} \tag{3A}$$

$$S_{ij} = \sigma_{ij} - \frac{1}{3}\sigma_{kk}\delta_{ij} \tag{4A}$$

$$a_{ij} = \alpha_{ij} - \frac{1}{3}\alpha_{kk}\delta_{ij} \tag{5A}$$

$$F = \frac{J_2}{k^2} - 1 \tag{6A}$$

$$G = \frac{I_2}{k_o^2} \tag{7A}$$

$$J_2 = \frac{1}{2} \xi_{ij} \xi_{ij} \tag{8A}$$

$$I_2 = \frac{1}{2} a_{ij} a_{ij} \tag{9A}$$

Here, $\dot{\varepsilon}_{ij}$ denotes the components of inelastic strain rate, k and α_{ij} are state variables and μ, n, m, β, R and H are material parameters. Specification of the evolutionary law for the scalar state variable k is made in the foregoing text. k_o is the value of k at the reference temperature T_o. It is assumed that all of the temperature dependence in the flow law, equations (1A), resides in the state variable k. Although this assumption is adequate for present purposes, a more generally valid representation might allow temperature dependence of the material parameters μ and n, as well. The recovery parameter R is taken as being strongly temperature dependent as as indicated below.

Values of the material parameters used in the present calculations are:

$$\mu = 3.6 \times 10^7$$

$$n = 4.0$$

$$\beta = 0.75$$

$$m = 3.87$$

$$R = 8.97 \times 10^{-8} \quad \exp[Q_R(1/T_o - 1/T)]$$

$$H = 9.92 \times 10^3$$

These are consistent with the units of ksi for stress, in/in for strain, time in hours and temperature in degrees Kelvin. The "activation energy" $Q_R = 4 \times 10^4$ and the reference temperature $T_o = 800K$.

The values of the material parameters stated above were determined for a common steel (2 1/4 Cr-1Mo), however, they are used here in the spirit of qualitatively representing a generic solid solution hardening alloy.

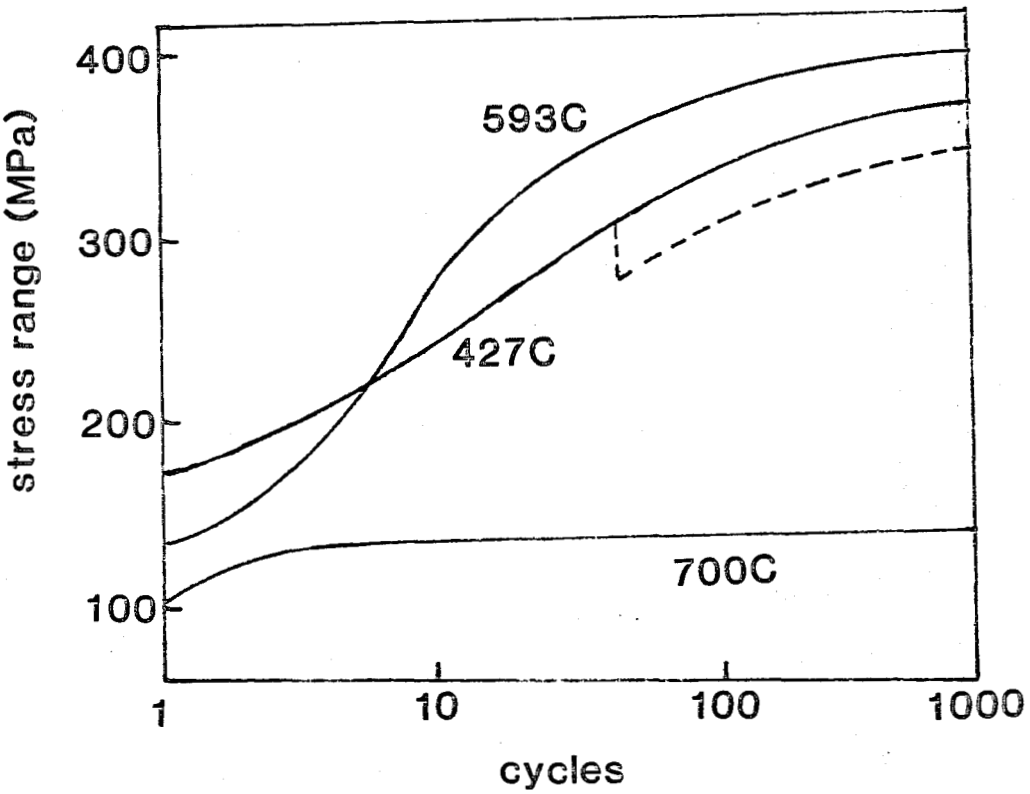

Figure 1 Isothermal cycling (solid lines) on type 304 stainless steel at 427, 593 and 700°C. Strain range is 0.54% and strain rate is 0.0001/s. Nonisothermal curve (dotted) shows cycling initially at 427°C changed to 593°C.

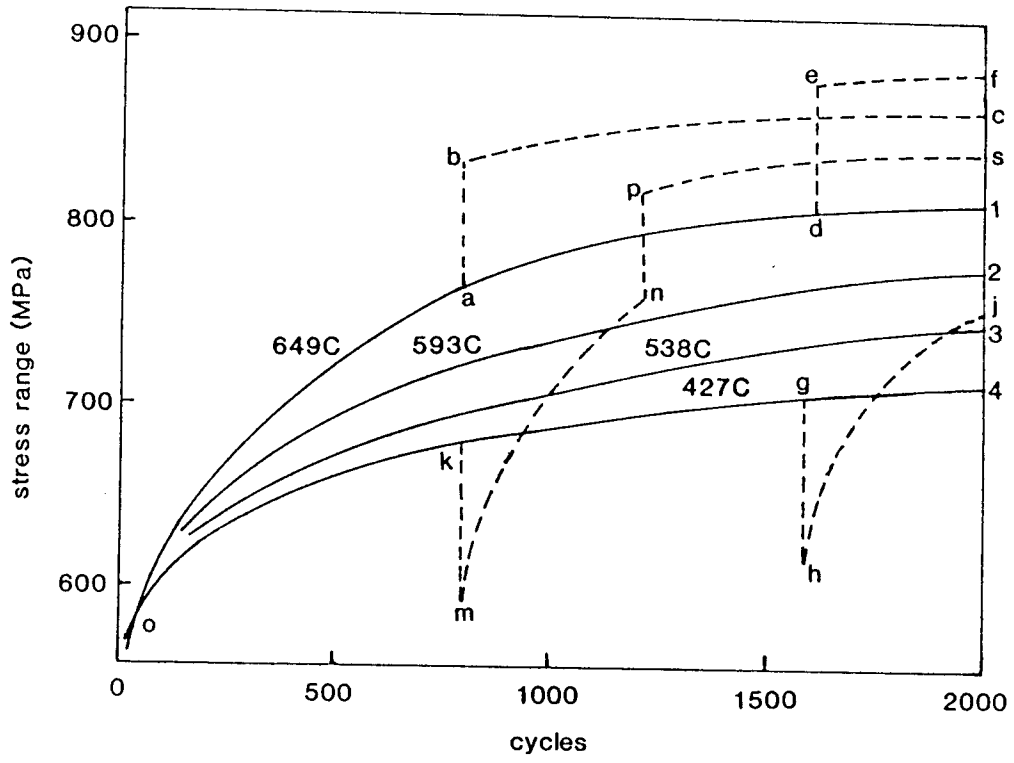

Figure 2 Isothermal cycling (solid lines) on Hastelloy X at 427, 538, 593 and 649°C. Strain range is 0.6% and strain rate is 0.001/s. Nonisothermal curves (dotted) obtained by cycling at 427°C and 649°C (see text).

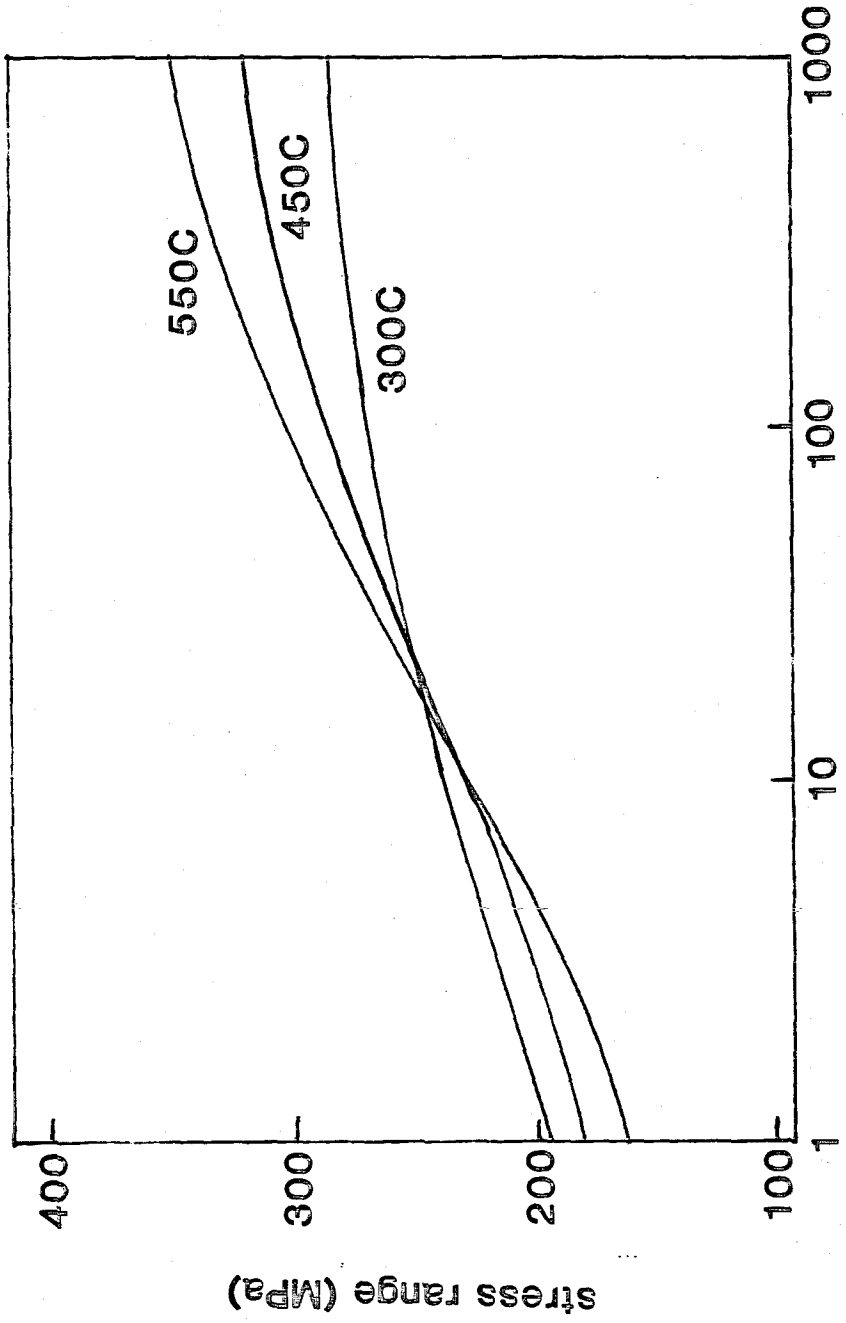

Figure 3 Isothermal cycling on type 316 stainless steel at 350, 450 and 550°C. Strain range is 0.56% and strain rate is 0.001/s.

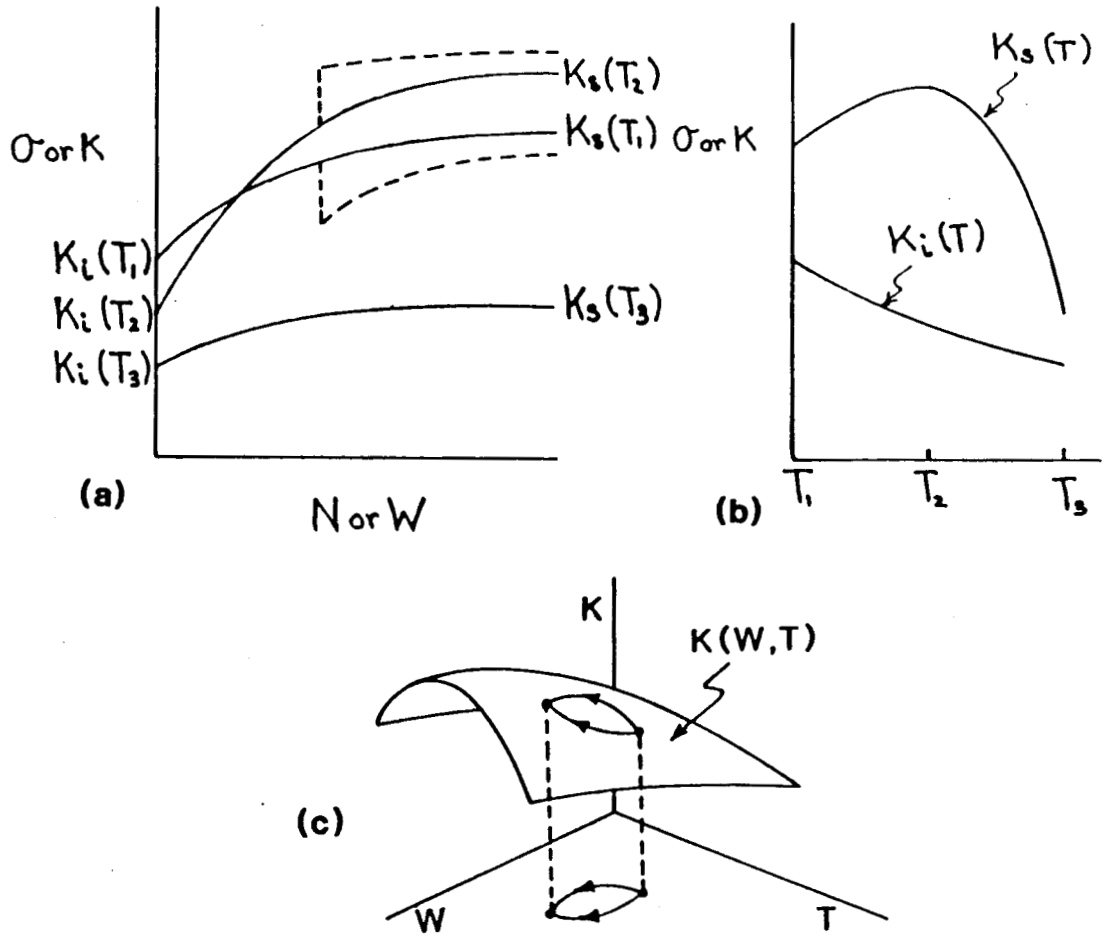

Figure 4 a) Typical isothermal (solid) and nonisothermal (dotted) hardening curves.
b) Typical hardening vs. temperature curve showing strain aging peak.
c) Surface k(W,T)

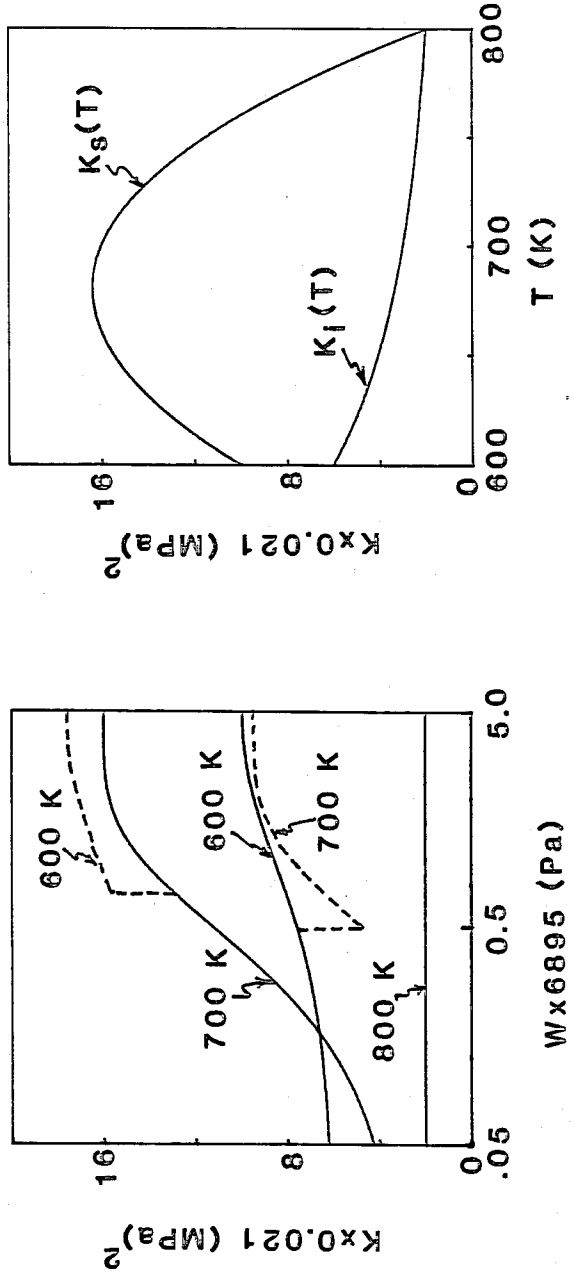

Figure 5 Isothermal hardening curves (solid lines) at 600, 700 and 800 k for models A and B. Nonisothermal curves (dotted lines) corresponding to model B only.

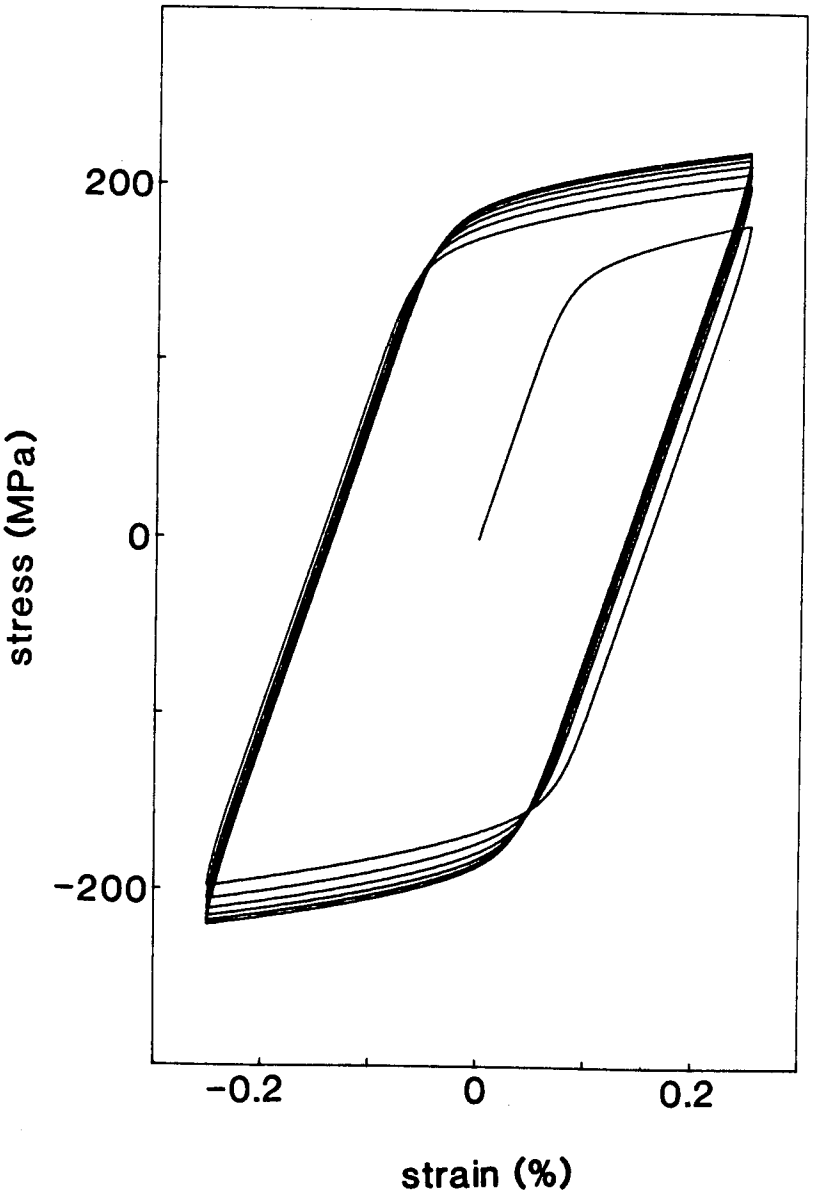

Figure 6 Isothermal hysteresis loop predicted by models A and B at 600 k. Strain range is 0.5%, strain rate is 0.004/m.

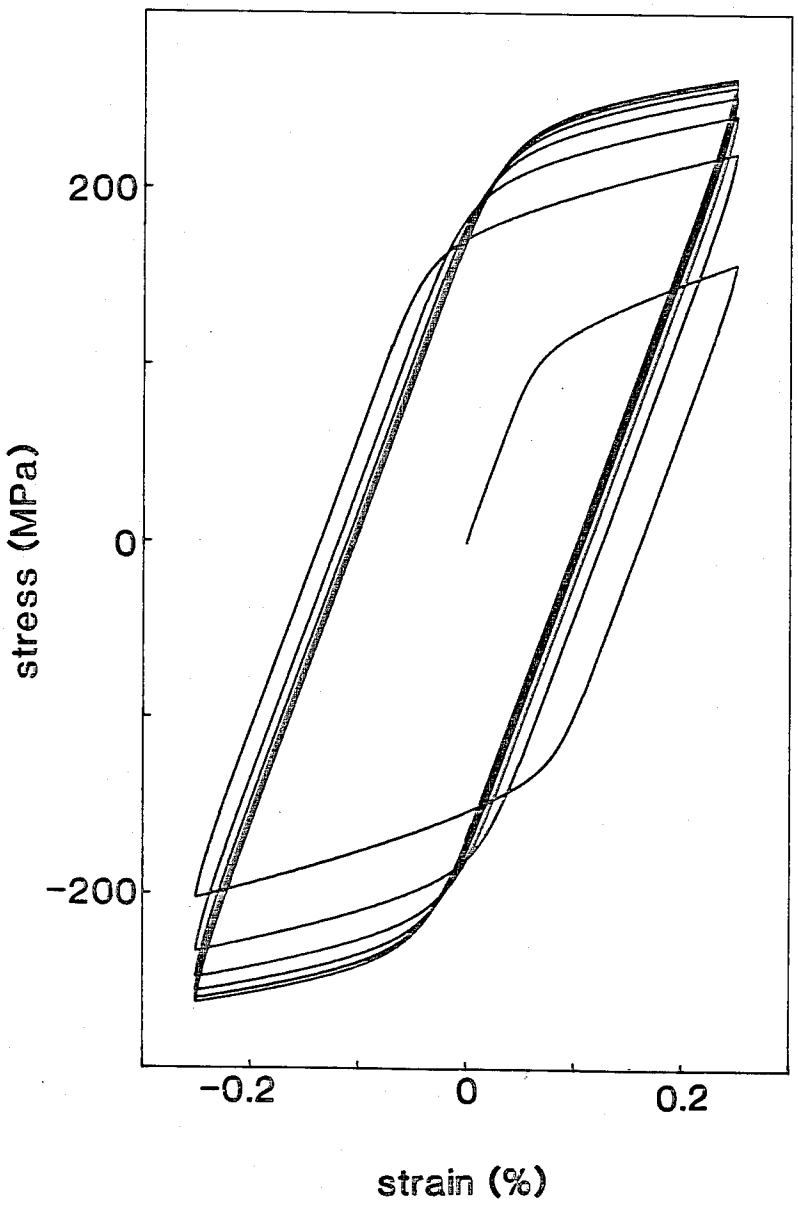

Figure 7 Isothermal hysteresis loop predicted by models A and B at 700 k. Strain range is 0.5%, strain rate is 0.004/m.

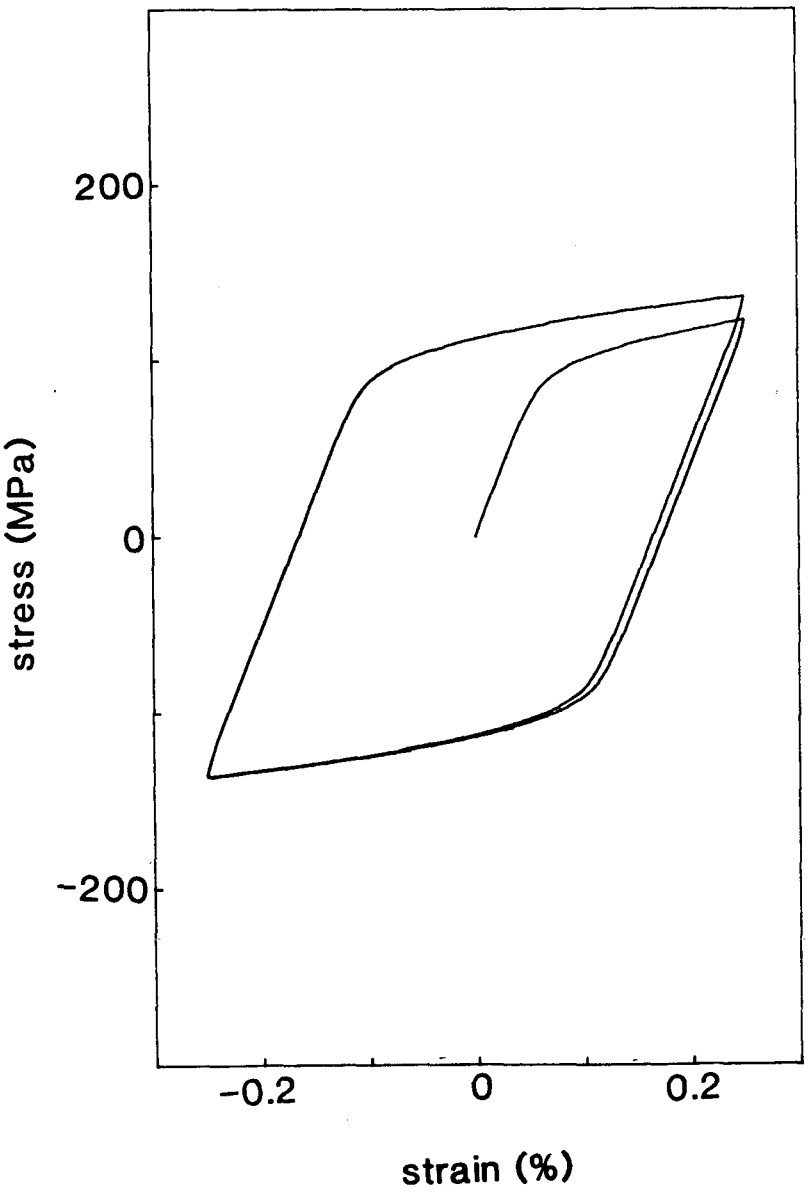

Figure 8 Isothermal hysteresis loop predicted by models A and B at 800 K. Strain range is 0.5%, strain rate is 0.004/m.

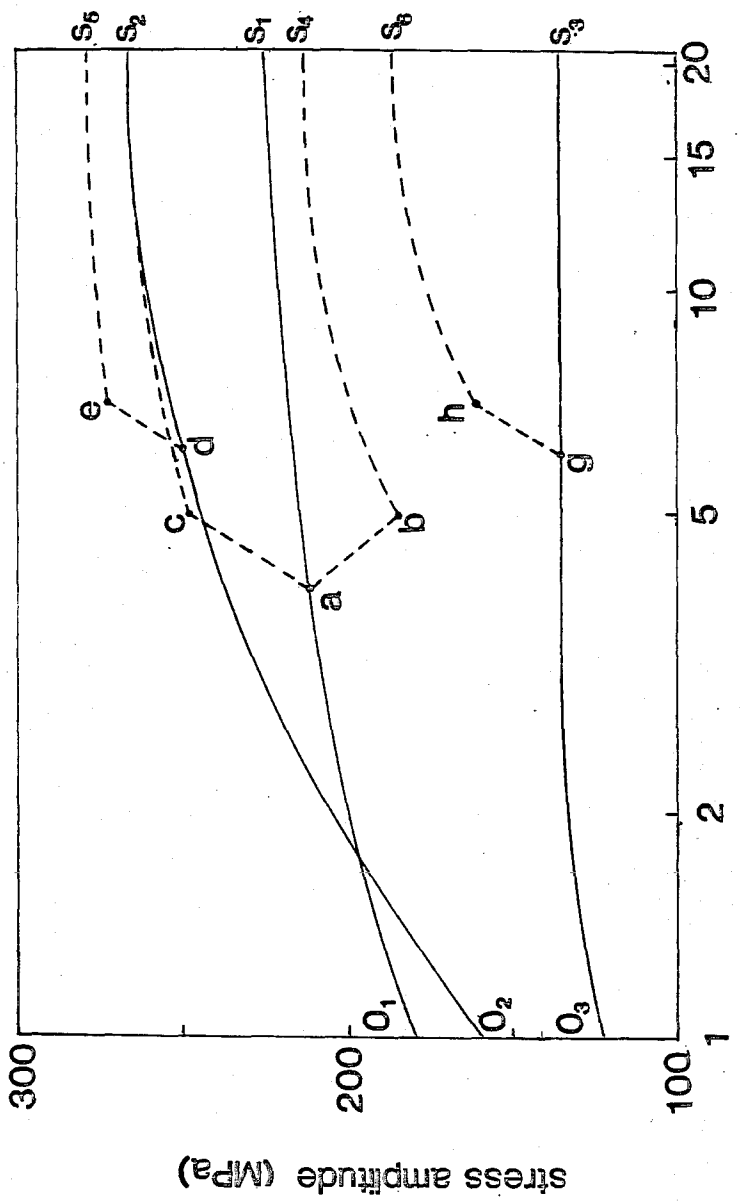

Figure 9 Isothermal cyclic hardening curves (solid) at 600 k (O_1S_1) 700 k (O_2S_2) and 800 k (O_3S_3) under conditions specified in figures 6-8. Dotted curves depict nonisothermal responses of models A and B (see text).

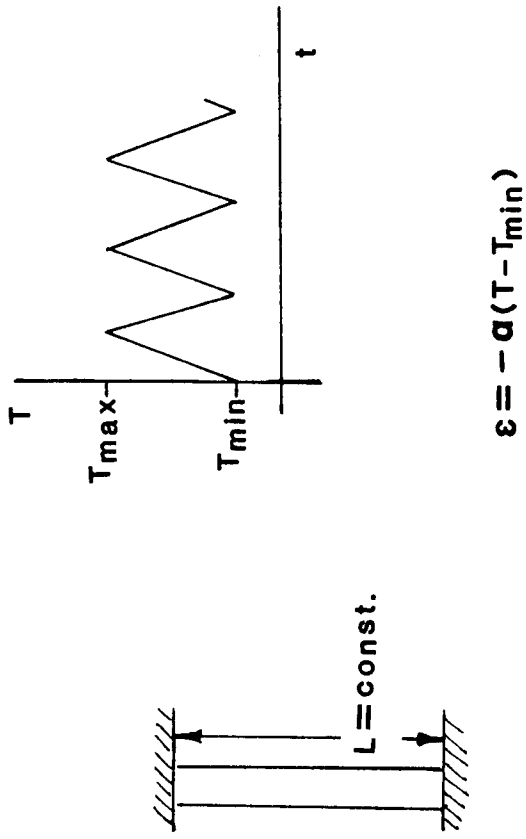

Figure 10 Thermal cycling of a fully constrained bar.

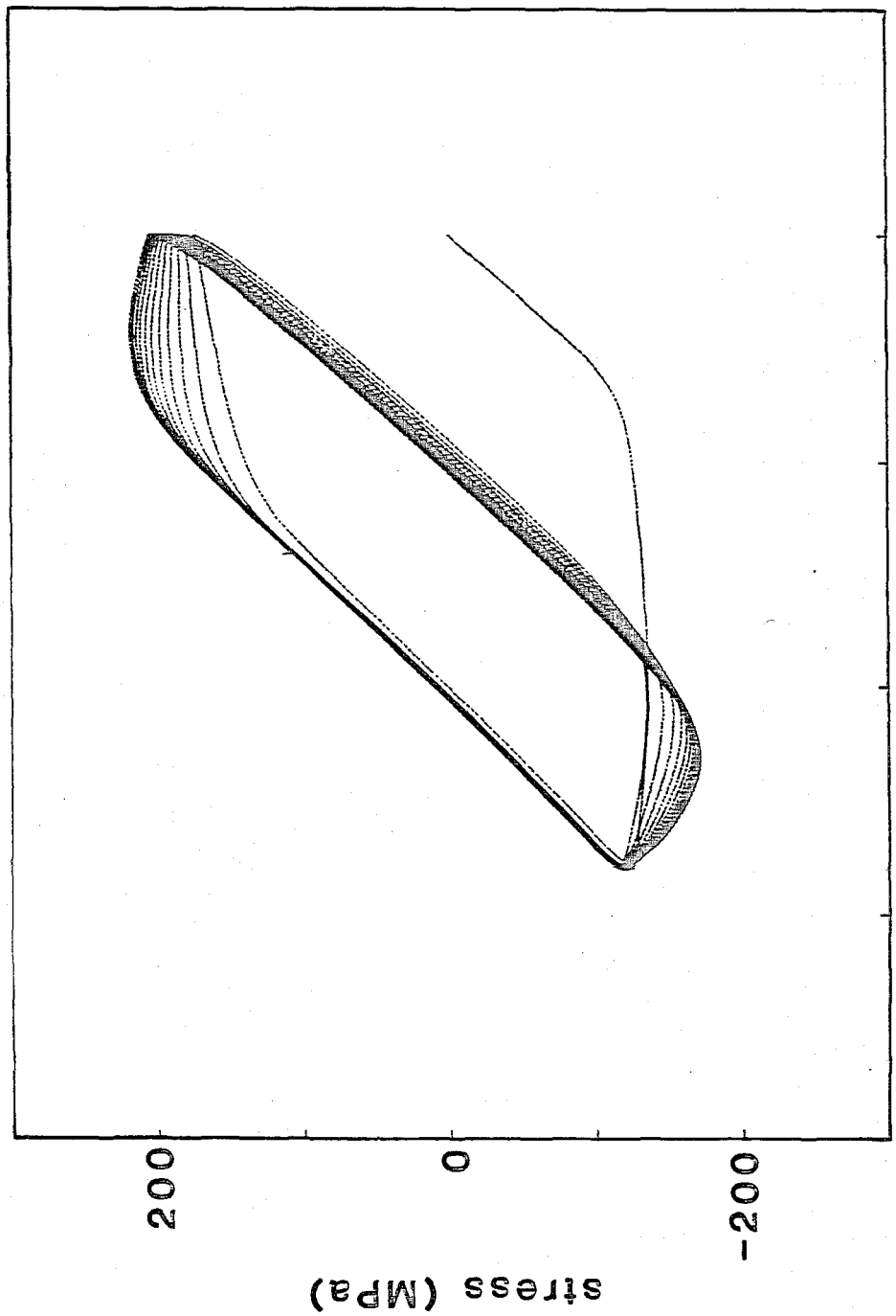

Figure 11 Response predicted by model A for thermal cycling over 600 - 800 K at 5K/s.

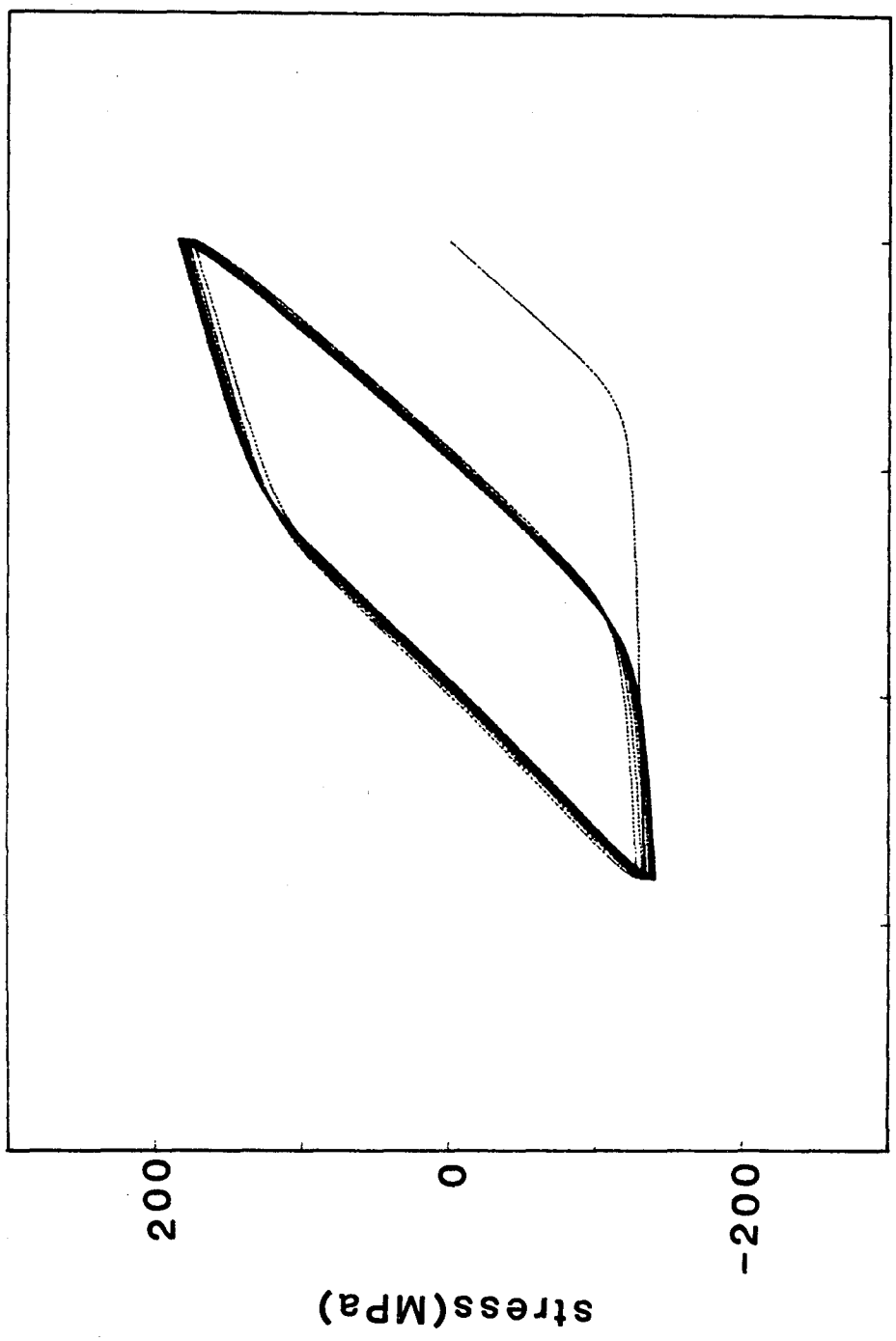

Figure 12 Response predicted by model B for thermal cycling over 600 - 800 k at 5k/s.

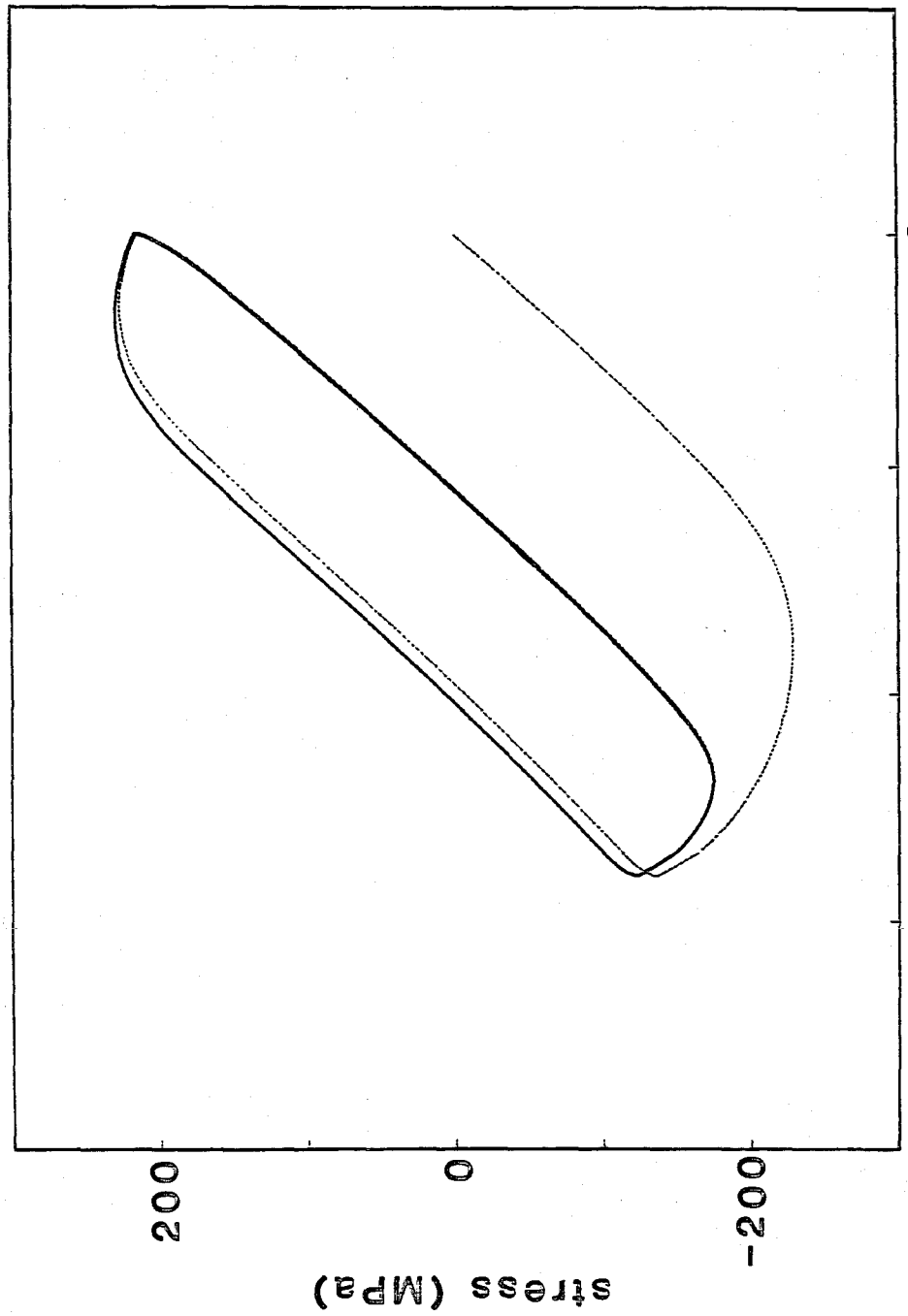

Figure 13 Response predicted by model A for thermal cycling over 600 - 800 k at 5k/s including only saturated isothermal information.

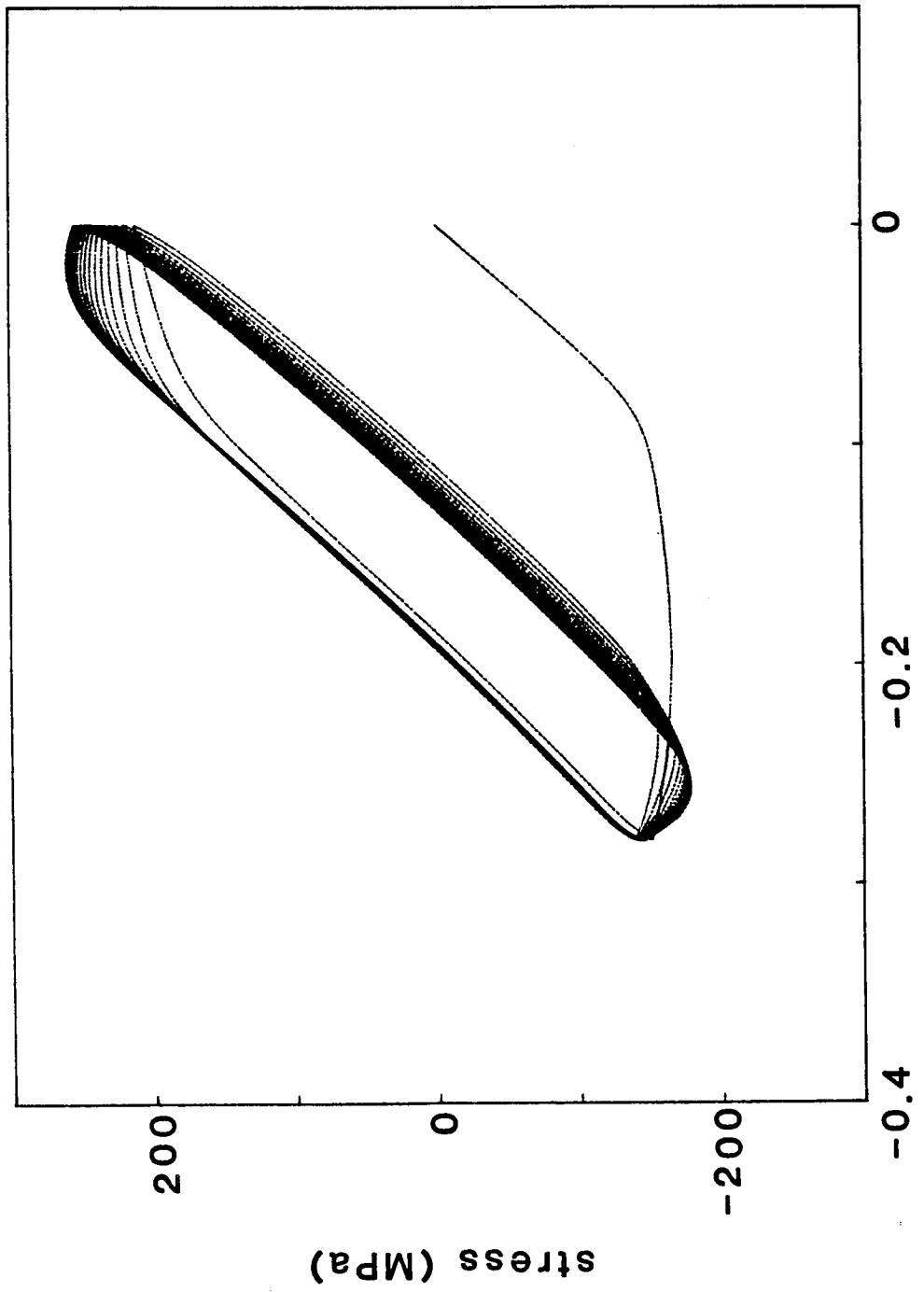

Figure 14 Response predicted by model A for thermal cycling over 600 -800 k at 50k/s.

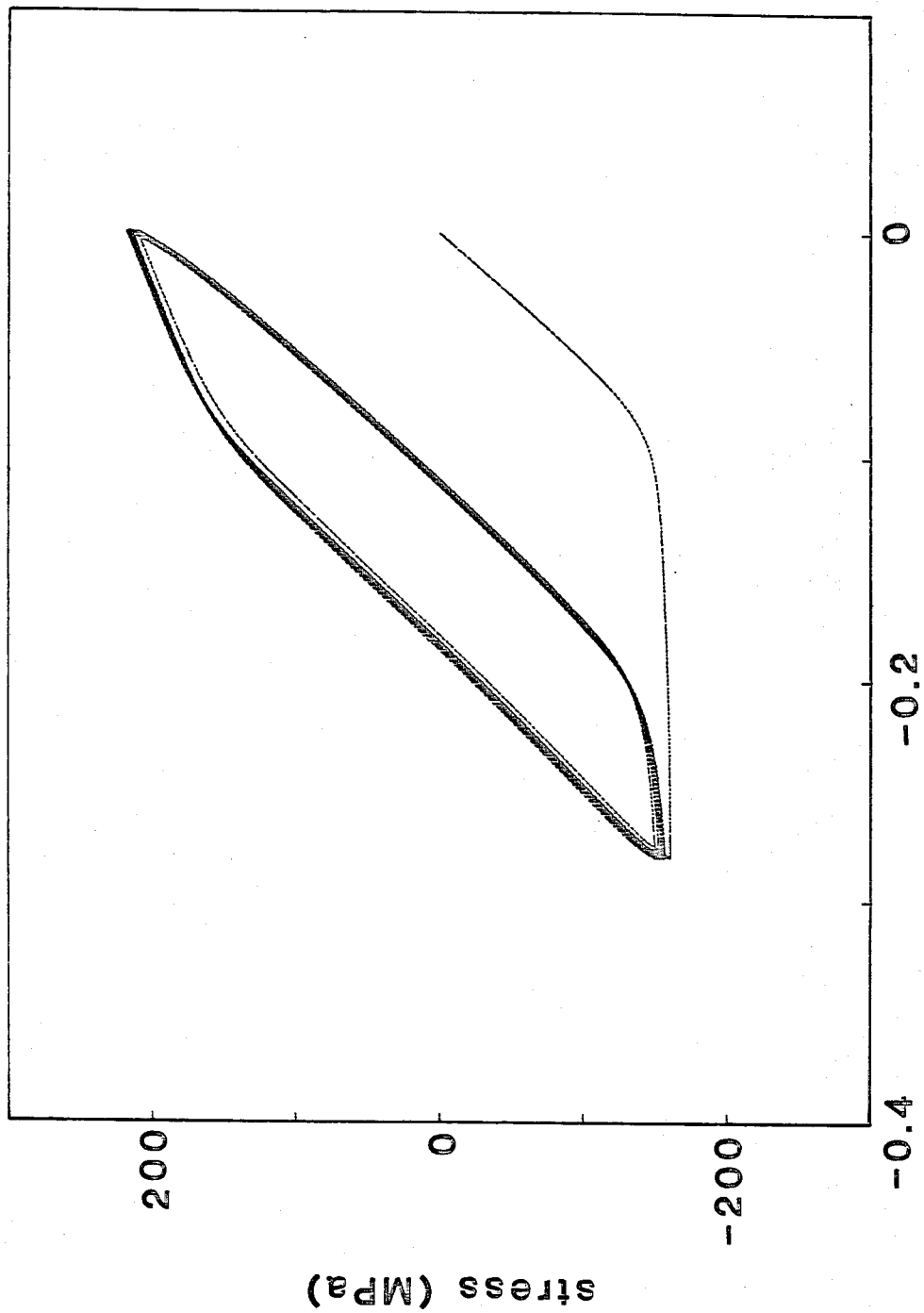

Figure 15 Response predicted by model B for thermal cycling over 600 - 800 k at 50k/s.

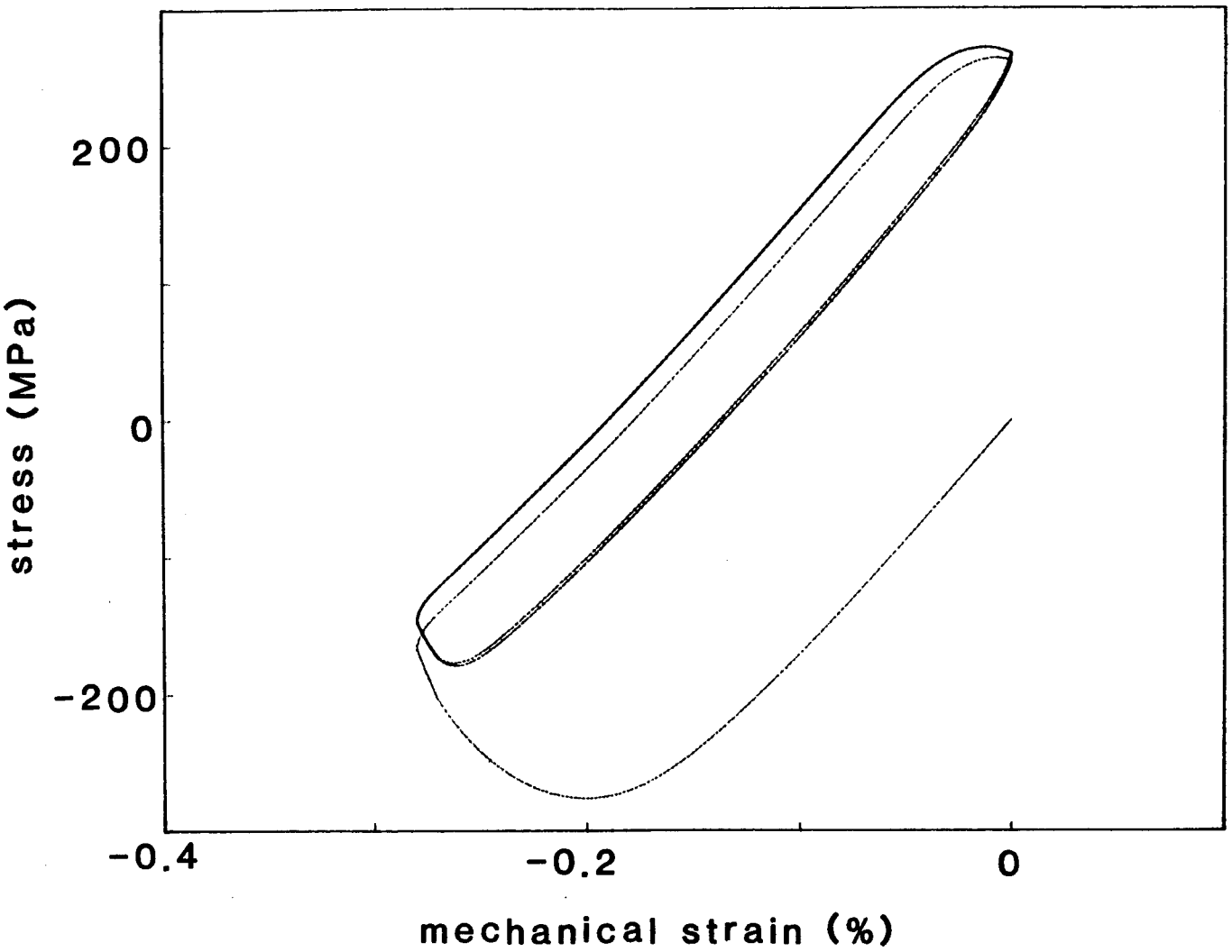

Figure 16 Response predicted by model A for thermal cycling over 600 -800 k at 50k/s including only isothermally saturated information.

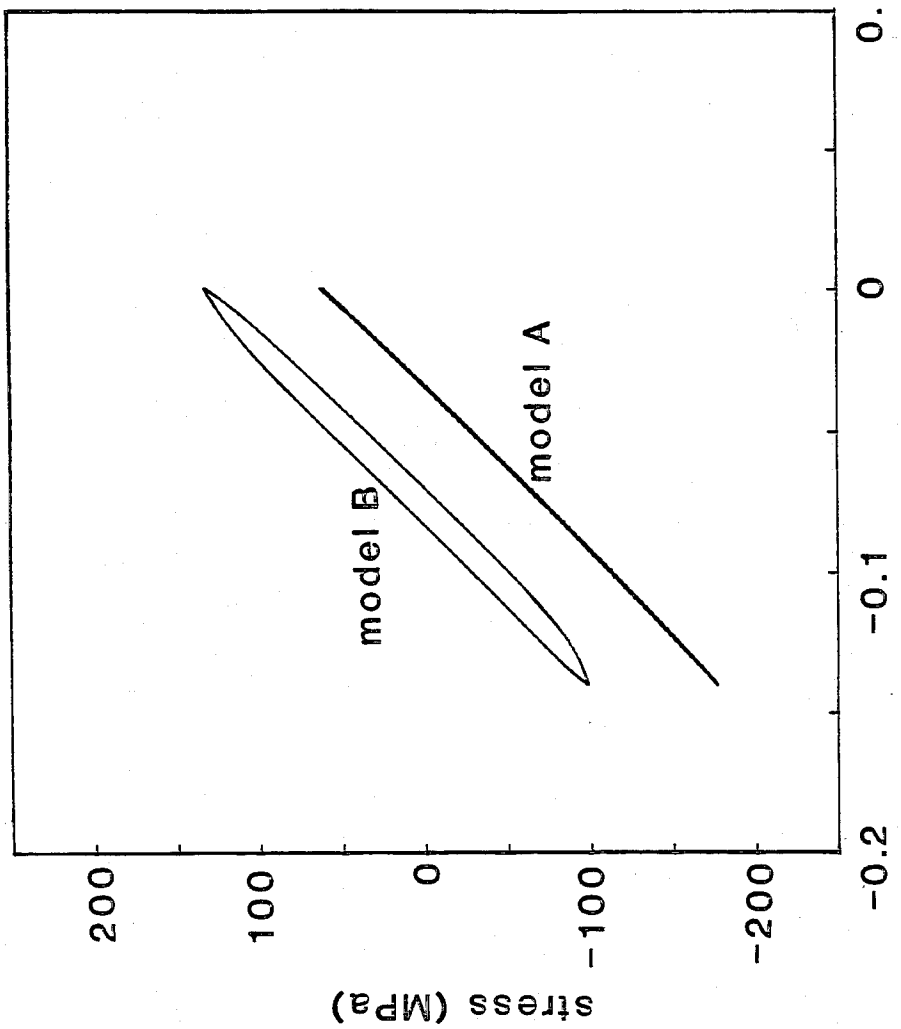

Figure 17 Comparison of stable hysteresis loops predicted by models A and B for thermal cycling over 600 - 700 k at 5k/s. Model A contains only isothermally saturated information.

1. Report No.	2. Government Accession No.	3. Recipient's Catalog No.
NASA CR-174836		

4. Title and Subtitle	5. Report Date
Viscoplastic Constitutive Relationships with Dependence on Thermomechanical History	March 1985
	6. Performing Organization Code

7. Author(s)	8. Performing Organization Report No.
D.N. Robinson and P.A. Bartolotta	None
	10. Work Unit No.

9. Performing Organization Name and Address	11. Contract or Grant No.
The University of Akron Dept. of Civil Engineering Akron, Ohio	NAG 3-379
	13. Type of Report and Period Covered
12. Sponsoring Agency Name and Address	Contractor Report
National Aeronautics and Space Administration Washington, D.C. 20546	14. Sponsoring Agency Code
	533-04-12

15. Supplementary Notes

Final report. Project Manager, Daniel J. Gauntner, Structures Division, NASA Lewis Research Center, Cleveland, Ohio 44135.

16. Abstract

Experimental evidence of thermomechanical history dependence in the cyclic hardening behavior of some common high-temperature structural alloys is presented with special attention paid to the contribution of dynamic metallurgical changes. A discussion is given concerning the inadequacy of formulating "non-isothermal" constitutive equations solely on the basis of isothermal testing. A representation of thermoviscoplasticity is proposed that qualitatively accounts for the observed hereditary behavior. This is achieved by formulating the scalar evolutionary equation in an established viscoplastic theory to reflect thermomechanical path dependence. Although the necessary nonisothermal tests for further quantifying the thermoviscoplastic model have been identified, such data are not yet available. To assess the importance of accounting for thermomechanical history dependence in practical structural analyses, two qualitative models are specified; the first is formulated as if based entirely on isothermal information, as is most often done; the second is made to reflect thermomechanical path dependence using the proposed thermoviscoplastic representation. Comparisons of prediction of the two models are made and a discussion is given of the impact the calculated differences in deformation behavior may have on subsequent lifetime predictions.

17. Key Words (Suggested by Author(s))	18. Distribution Statement
Viscoplasticity Thermomechanical Constitutive theory	Unclassified - unlimited STAR Category 39

19. Security Classif. (of this report)	20. Security Classif. (of this page)	21. No. of pages	22. Price*
Unclassified	Unclassified	40	

*For sale by the National Technical Information Service, Springfield, Virginia 22161